Ultrasonics 86 (2018) 6–13

Contents lists available at ScienceDirect

Ultrasonics

journal homepage: www.elsevier.com/locate/ultras

Influence of electrical boundary conditions on profiles of acoustic field and electric potential of shear-horizontal acoustic waves in potassium niobate plates

I.E. Kuznetsova [a,*], I.A. Nedospasov [a], V.V. Kolesov [a], Z. Qian [b,*], B. Wang [b], F. Zhu [b]

[a] Kotelnikov Institute of Radio Engineering and Electronics of RAS, Moscow 125009, Russia
[b] Nanjing University of Aeronautics and Austronautics, SKL of MCMS, Nanjing, China

ARTICLE INFO

Article history:
Received 21 August 2017
Received in revised form 14 January 2018
Accepted 17 January 2018

Keywords:
Acoustic field profile
Electric potential distribution
Forward and backward plate acoustic waves
Potassium niobate
Electrical boundary conditions
Phase and group velocity
Arbitrary conductive layer

ABSTRACT

The profiles of an acoustic field and electric potential of the forward and backward shear-horizontal (SH) acoustic waves of a higher order propagating in X-Y potassium niobate plate have been theoretically investigated. It has been shown that by changing electrical boundary conditions on a surface of piezoelectric plates, it is possible to change the distributions of an acoustic field and electric potential of the forward and backward acoustic waves. The dependencies of the distribution of a mechanical displacement and electrical potential over the plate thickness for electrically open and electrically shorted plates have been plotted. The influence of a layer with arbitrary conductivity placed on a one or on the both plate surfaces on the profiles under study, phase and group velocities of the forward and backward acoustic waves in X-Y potassium niobate has been also investigated. The obtained results can be useful for development of the method for control of a particle or electrical charge movement inside the piezoelectric plates, as well a sensor for definition of the thin film conductivity.

1. Introduction

It is known that the forward and backward acoustic waves can propagate in piezoelectric plates [1–5]. In contrast to the forward acoustic waves the backward ones exhibit oppositely directed phase and group velocities. These waves possesses unique properties and there are many paper devoted to their study [6–8]. It has been previously shown that not only Lamb waves, but also shear-horizontal acoustic waves can be backward in piezoelectric plates under certain conditions [4,9]. However, the SH backward waves disappear if piezoelectricity is ignored in the crystal [9]. The study of the conditions of propagation of the backward acoustic waves in piezoelectric plates has been continued in Ref. [4]. Here the dependencies of mechanical displacement components for forward and backward waves over the depth of X-Y + 30 $KNbO_3$ plate were obtained and analyzed. The results of examination of the peculiarities of propagation and hybridization of the backward Lamb modes in lithium niobate and potassium niobate plates are presented in Refs. [4,10]. In the paper [11] the mechanisms of an appearance and existence of the pure shear backward waves and waves with zero group velocity in the plates of X- and Y-cuts of a rhombic potassium niobate crystal showing an extremely strong piezoeffect were considered [12,13].

It is known that the acoustic waves are characterized not only phase and group velocities and attenuation but also so-called a wave structure or displacement profile [14–18]. The information about relation between the mechanical displacement components on the waveguide surface is very important for the choosing type of an operating wave at the development of various sensors. For example, for the development of liquid sensors it is necessary to use the waves with the minimum mechanical displacement perpendicular to a plate surface [19–21]. Such waves propagate practically without attenuation in the presence of liquid [14,22]. The information about the value of an electric potential on the plate surface is valuable, for example, for the development of the non-contact methods for determination of thin film conductance and permittivity [23], for analysis of the heterostructures and conductivity mechanisms [24,25]. In these cases the influence of the electric boundary conditions on the properties of the acoustic waves in the piezoelectric waveguides is used. It is necessary to note that there are a lot of the papers devoted to the investigation of the

* Corresponding authors at: Kotelnikov Institute of Radio Engineering and Electronics of RAS, Mokhovaya 11, bld.7, Moscow 125009, Russia (I.E. Kuznetsova). State Key Laboratory of Mechanics and Control of Mechanical Structures/College of Aerospace Engineering, Nanjing University of Aeronautics and Astronautics, Nanjing, China (Z. Qian).

E-mail addresses: kuziren@yandex.ru (I.E. Kuznetsova), qianzh@nuaa.edu.cn (Z. Qian).

https://doi.org/10.1016/j.ultras.2018.01.010
0041-624X/

influence of different electrical boundary conditions (metallization of a surface, placement of a layer with arbitrary conductivity or conductive liquid on the surface, the approaching metal layer to surface, etc.) on the velocity and attenuation of various types of acoustic waves [26–33]. In Ref. [27] the effect of the metallization of one or both plate sides on the distribution of the mechanical displacements of the quasi-longitudinal QL waves over the 128Y-X + 90 $LiNbO_3$ plate thickness has been theoretically and experimentally investigated. In Ref. [32] the influence of the distance between ideally conductive plane and Y-X + 15 $KNbO_3$ crystal surface on the relation of the mechanical displacement components has been considered. In Ref. [33] it has been theoretically shown that different electrical boundary conditions have an influence on the second-harmonic generation effect of ultrasonic guided wave propagation in piezoelectric plates.

In whole, the obtained results have shown that the electrical boundary conditions impact on the distribution of the mechanical displacement components in piezoelectrics. However the study of the influence of various electrical boundary conditions on the distribution of an electric potential over the plate thickness has not yet been carried out. It is known only from Refs. [34–37], where the influence of electrical boundary conditions on the potential distribution of Bleustein-Gulyaev waves over the depth of piezoelectric crystal was investigated. The obtained results allowed to reveal the physical reasons of the anomalous resisto-acoustic effect and conditions of its existence.

As for backward acoustic waves in piezoelectric plates the papers devoted to the investigation of its acoustic field profiles and electric potential distributions over the plate thickness are practically absent. On this basis, the aim of this paper is to theoretically study the effect of different electrical boundary conditions for X-Y potassium niobate plate on the acoustic field profiles and electric potential distributions of the forward and backward shear-horizontal acoustic waves. Such electrical boundary conditions include (i) metallization of one or both sides of the piezoelectric plate, (ii) placement of a layer with arbitrary conductivity on one or both sides of the piezoelectric plate.

2. Theoretical analysis

Let us consider the propagation of the SH forward and backward acoustic waves in X-Y potassium niobate plate (Euler angles 90, 90, 0) [38]. Fig. 1 shows the problem geometry. The wave always propagates along the x_1- axis of a piezoelectric plate bounded by $x_3 = 0$ and $x_3 = h$ planes. The cristallophysics material constants are recalculated into our coordinate system by using Euler angles [38].

Regions $x_3 < 0$ and $x_3 > h$ contain vacuum. We consider a two dimensional problem and all mechanical and electrical variables are assumed to be constant in the x_2-axis direction in this case. To solve the problem we write motion equation, Laplace equation, and material equations for piezoelectric medium using the quasi-electrostatic approximation $E_i = \partial\Phi/\partial x_i$ [39]:

$$\rho\partial^2 U_i/\partial t^2 = \partial T_{ij}/\partial x_j, \quad \partial D_j/\partial x_j = 0, \tag{1}$$

$$T_{ij} = C_{ijkl}\partial U_l/\partial x_k + e_{kij}\partial\Phi/\partial x_k, \quad D_j = -\varepsilon_{jk}\partial\Phi/\partial x_k + e_{jlk}\partial U_l/\partial x_k. \tag{2}$$

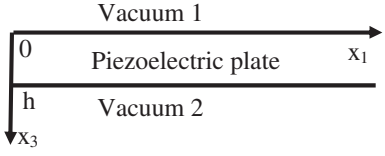

Fig. 1. Geometry of the task.

Here, E_i, U_i, t, T_{ij}, x_j, D_j, Φ, ρ, C_{ijkl}, e_{ikl}, and ε_{jk} are the components of the electric field, mechanical particle displacement, time, the components of mechanical stress tensor, coordinates, the components of electric displacements, electric potential, and density, as well elastic, piezoelectric and dielectric constants of a piezoelectric, respectively.

Outside the plate in $x_3 < 0$ and $x_3 > h$ regions, electric displacement should satisfy the Laplace equation:

$$\partial D_j^{v_1}/\partial x_j = 0, \quad \partial D_j^{v_2}/\partial x_j = 0, \tag{3}$$

where $D_j^{v_1} = -\varepsilon_0\partial\Phi^{v_1}/\partial x_j$ and $D_j^{v_2} = \varepsilon_0\partial\Phi^{v_2}/\partial x_j$. Here, indexes v_1 and v_2 denotes quantities relating to vacuum in the planes $x_3 = 0$ and $x_3 = h$, respectively, ε_0 is the dielectric constant of vacuum.

Acoustic waves propagating in the plate should satisfy, as well, mechanical and electrical boundary conditions. At the boundary with vacuum ($x_3 = 0$ and $x_3 = h$), these conditions have the following view:

$$T_{3j} = 0, \quad \Phi^{v_1} = \Phi, \quad \Phi^{v_2} = \Phi, \quad D_3^{v_1} = D_3, \quad D_3^{v_2} = D_3. \tag{4}$$

Potential becomes zero when the plate is short-circuited with an infinitely thin metal layer from a one ($x_3 = h$) or the two ($x_3 = 0$ and $x_3 = h$) sides.

In the case of presence of a thin layer with arbitrary conductivity at the boundary with vacuum ($x_3 = h$) the corresponding electrical boundary conditions have the following form [36]:

$$\Phi^{v_2} = \Phi; \quad D_3^{v_2} - D_3 = \delta. \tag{5}$$

Here, δ is the surface charge density that is related to the density of surface current. The equation of charge conservation can be written in the next form [39]

$$\partial J_1^{lr}/\partial x_1 = \partial\delta/\partial t. \tag{6}$$

Here, J_1^{lr} is the component of surface current density ($x_3 = h$).

Hence it follows, regarding the expression for the surface current conductivity in the layer [39]:

$$J_1^{lr} = \sigma_S\partial\Phi^{v_2}/\partial x_1, \tag{7}$$

and taking into account that all variables are proportional to $\exp(j\omega(t - x_1/V))$ one can obtain

$$\delta = j\sigma_S\Phi^{v_2}\omega/V^2. \tag{8}$$

Here, σ_S is the surface conductance of the layer, j is the imaginary unit, V is the phase velocity of the acoustic wave.

The electrical boundary conditions are changed in the case of presence of a thin layers with arbitrary conductivity on both sides of the plate with vacuum ($x_3 = 0$ and $x_3 = h$) and can be written as:

$$\Phi^{v_1} = \Phi, \quad D_3^{v_1} - D_3 = -\delta, \quad \Phi^{v_2} = \Phi, \quad D_3^{v_2} - D_3 = \delta. \tag{9}$$

The above mentioned boundary problems were solved numerically by using the iterative procedure described in [36].

In result the values of the phase and group velocities, attenuation and amplitudes for all electrical and mechanical variables as functions of coordinate x_3 were obtained.

The presence of the conducting layer on the plate surface leads to the attenuation of the acoustic waves [28,29,36]. In this case the value of imaginary part of velocity becomes much higher than zero and we used the next expression for phase velocity calculation [40]:

$$V_{ph} = (\mathrm{Re}(V_{ph})^2 + \mathrm{Im}(V_{ph})^2)/\mathrm{Re}(V_{ph}) \tag{10}$$

Here $\mathrm{Re}(V_{ph})$ and $\mathrm{Im}(V_{ph})$ are the real and imaginary parts of the phase velocity, respectively.

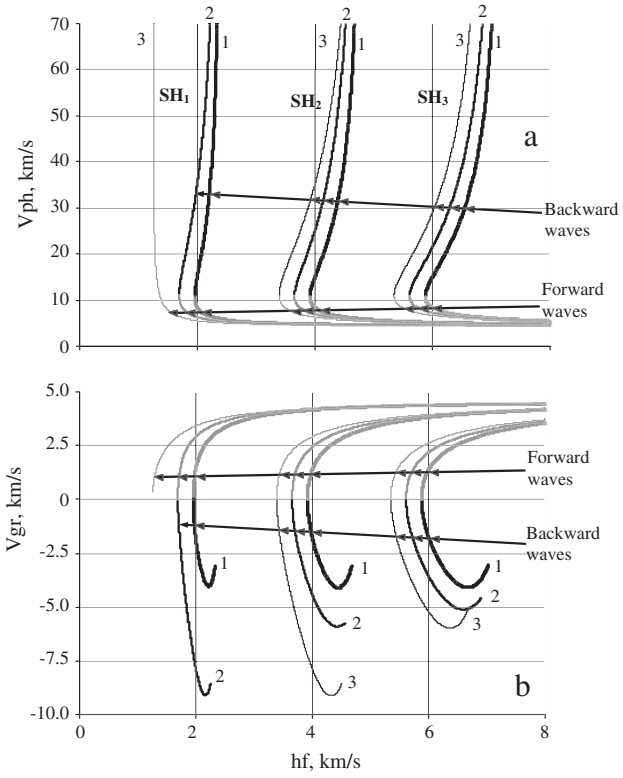

Fig. 2. Dependencies of phase (a) and group (b) velocities of forward (grey lines) and backward (black lines) SH_n waves in X-Y $KNbO_3$ plate on parameter hf: 1 – electrically open plate, 2 – plate electrically shorted from one side, and 3 – plate electrically shorted from two sides.

3. Results and discussion

3.1. Influence of metallization of a plate surface on the characteristics of forward and backward SH higher order acoustic waves in X-Y potassium niobate plate

As the result of the boundary problem solution, we have obtained the dependencies of phase velocities for the SH_n forward and backward acoustic waves of the n = 1, 2, and 3 orders propagating in X-Y potassium niobate plate on parameter hf (Fig. 2a). Here h and f are the plate thickness and wave frequency, respectively.

The material constants of potassium niobate were taken from Ref. [41]. At the first step calculations were performed for the electrically open plate (1), plate with one short-circuited surface (2) and plate with both electrically shorted surfaces (3).

The group velocities of the waves under study were calculated by using dispersion curves presented in Fig. 2a [11,38].

$$V_{gr} = d\omega/dk. \tag{11}$$

Here k is the real part of the wave number. The obtained dispersion curves are presented in Fig. 2b.

The analysis has shown that the point of the backward wave occurrence is shifted into the region of lower frequencies and the range of its existence increases under the plate metallization, which confirms with data cited in Ref. [5]. The SH_1 backward wave disappears under metallization of the two sides of the plate.

We also plotted the dependencies of electric potential value (upper row) and maximum mechanical displacement component U_2 (lower row) normalized to the value at the plate surface $U_{surf} = \sqrt{U_{1surf}^2 + U_{2surf}^2 + U_{3surf}^2}$ ($x_3 = 0$) for the backward (Fig. 3) and forward (Fig. 4) SH_1, SH_2, SH_3 acoustic waves on the plate thickness at hf_{SH1} = 2 km/s, hf_{SH2} = 4 km/s, hf_{SH3} = 6 km/s. As previously, the curves 1, 2, and 3 correspond to electrically open plate, plate electrically shorted from one and two sides, respectively.

It is seen that one would control both the magnitude of electric field associated with the acoustic wave, and the amplitude of particle displacement over the plate thickness. For experimental check of the theoretical results it is possible to use mesostructure based on a piezoelectric plate with through nanoholes. The direct measurement of the distribution and dynamic change of an internal electric field of a wave in such plate can be carried out by means of an electronic probe, for example, of an electronic microscope. By the changing the electrical boundary conditions on a plate surface it is possible to modulate this electronic stream by means of change of the built-in electric potential over plate depth. A nanoelectronic accelerator (modulator) of electrons based on such principle can be developed.

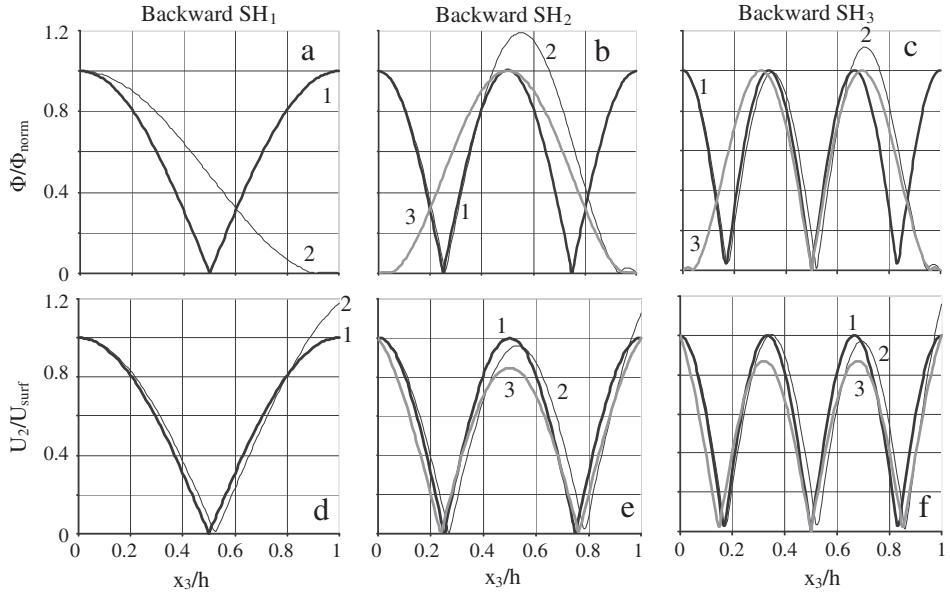

Fig. 3. Dependencies of the electric potential value (upper row) and maximum mechanical displacement component U_2 (lower row) normalized to the corresponding values at the plate surface ($x_3 = 0$) for backward SH_1 (a, d), SH_2 (b, e), SH_3 (c, f) waves on the thickness of X-Y $KNbO_3$ plate at hf_{SH1} = 2 km/s, hf_{SH2} = 4 km/s, hf_{SH3} = 6 km/s: 1 – electrically open plate, 2 – plate short-circuited from one side, and 3 – plate short-circuited from two sides.

For measuring backward-wave motions in plates it is also possible to use dynamic photoelastic technique [42].

For smooth change of electric boundary conditions it is possible to apply a layer whose conductivity can be changed by means of an external impact on a plate surface. It can be a semiconductor heterostructure controlled by applied electric field [43], or material whose conductivity changes under the influence of lighting (chromophores, photo-semiconductor structures) [44,45].

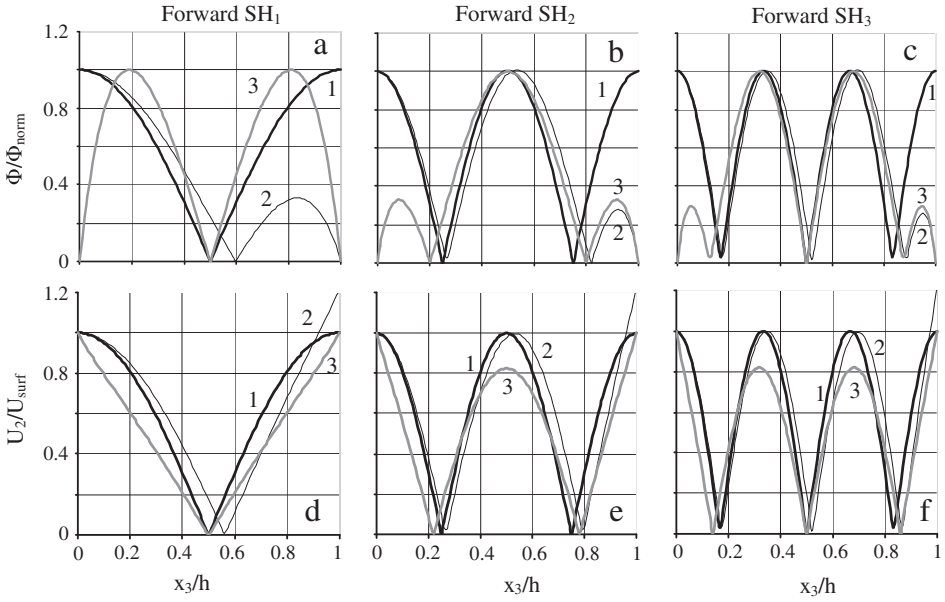

Fig. 4. Dependencies of the electric potential value (upper row) and maximum mechanical displacement component U_2 (lower row) normalized to the corresponding values at the plate surface ($x_3 = 0$) for forward SH_1 (a, d), SH_2 (b, e), SH_3 (c, f) waves on the thickness of X-Y $KNbO_3$ plate at $hf_{SH1} = 2$ km/s, $hf_{SH2} = 4$ km/s, $hf_{SH3} = 6$ km/s: 1 – electrically open plate, 2 – plate short-circuited from one side, and 3 – plate short-circuited from two sides.

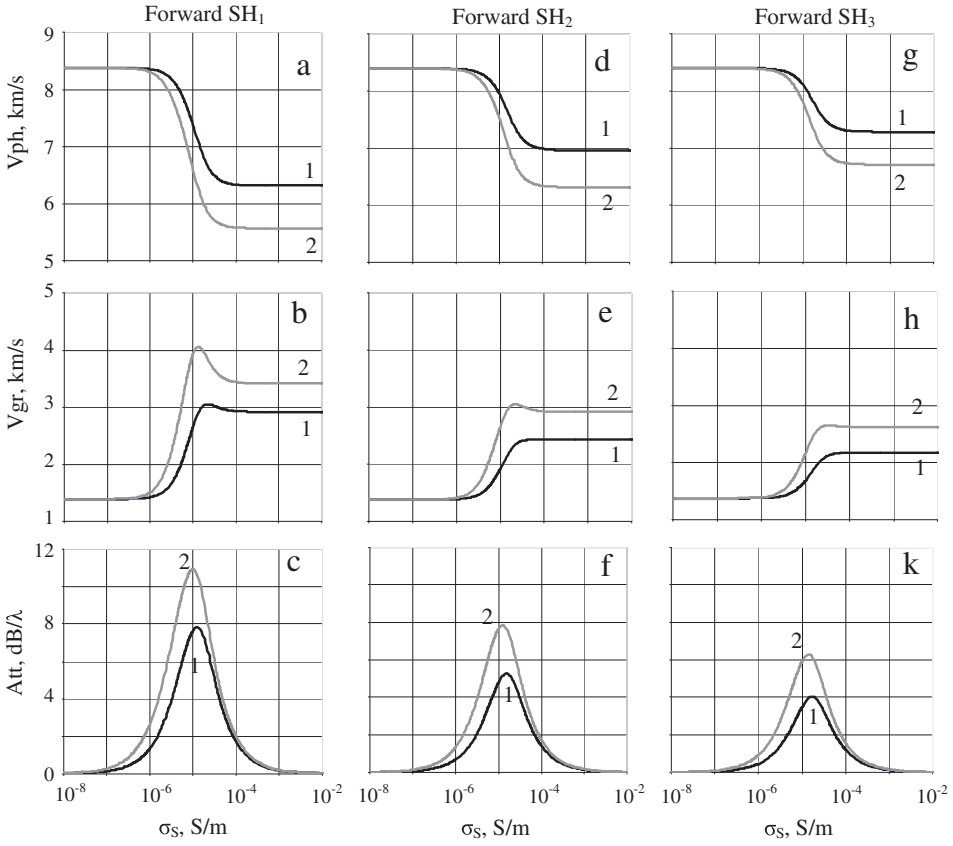

Fig. 5. Dependences of phase (upper row), group (middle row) velocities and attenuation (lower row) for the forward SH_1 (a, b, c), SH_2 (d, e, f), and SH_3 (g, h, k) acoustic waves at $hf_{SH1} = 2$ km/s, $hf_{SH2} = 4$ km/s, $hf_{SH3} = 6$ km/s propagating in the X-Y potassium niobate plate on surface conductivity σ_s: 1- a layer with σ_s is in plane $x_3 = h$, 2- layers with σ_s are in planes $x_3 = 0$ and $x_3 = h$.

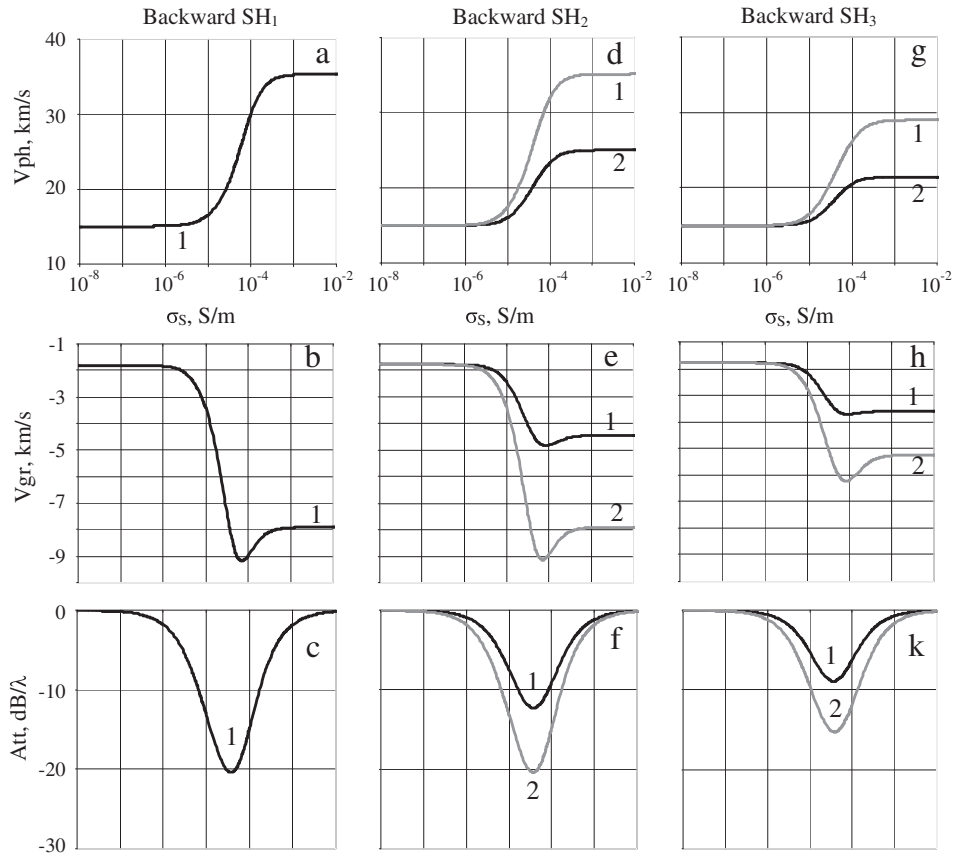

Fig. 6. Dependences of phase (upper row), group (middle row) velocities and attenuation (lower row) for the backward SH_1 (a, b, c), SH_2 (d, e, f), and SH_3 (g, h, k) acoustic waves at hf_{SH1} = 2 km/s, hf_{SH2} = 4 km/s, hf_{SH3} = 6 km/s propagating in the X-Y potassium niobate plate on surface conductivity σ_s: 1- a layer with σ_s is in plane $x_3 = h$, 2- layers with σ_s are in planes $x_3 = 0$ and $x_3 = h$.

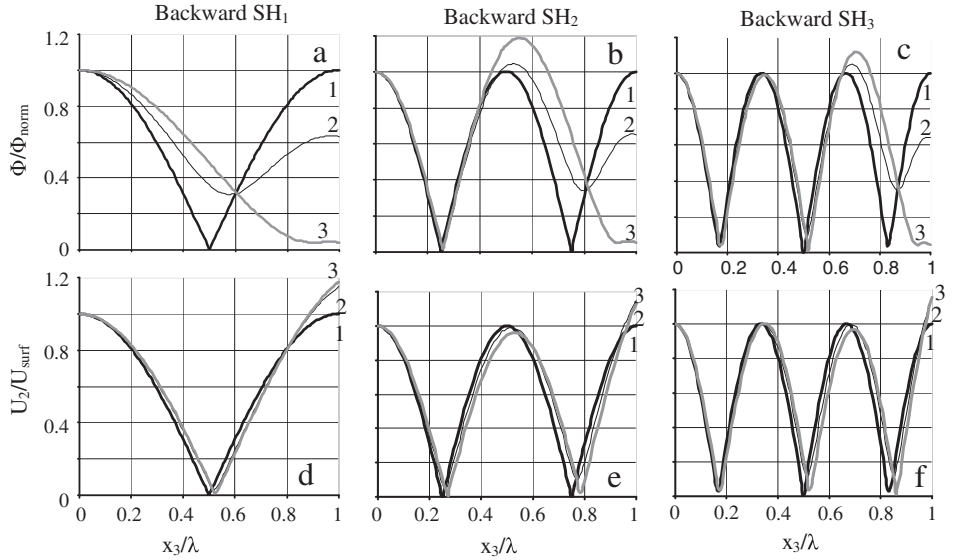

Fig. 7. Dependences of electric potential value (upper row) and maximum mechanical displacement component U_2 (lower row) normalized to the corresponding values at the plate surface ($x_3 = 0$) for backward SH_1 (a, d), SH_2 (b, e), SH_3 (c, f) waves on the thickness of XY $KNbO_3$ plate at hf_{SH1} = 2 km/s, hf_{SH2} = 4 km/s, hf_{SH3} = 6 km/s. The curves 1, 2, and 3 correspond to values $\sigma_s = 10^{-8}$ S/m, 5×10^{-5} S/m, and 10^{-3} S/m of the layer placed in plane $x_3 = h$, respectively.

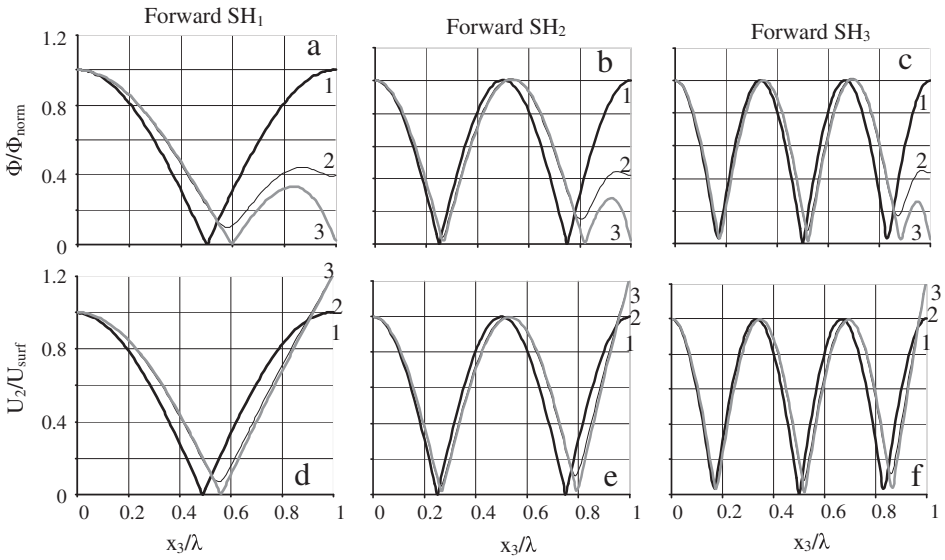

Fig. 8. Dependences of electric potential value (upper row) and maximum mechanical displacement component U_2 (lower row) normalized to the corresponding values at the plate surface ($x_3 = 0$) for forward SH_1 (a, d), SH_2 (b, e), SH_3 (c, f) waves on the thickness of XY $KNbO_3$ plate at $hf_{SH1} = 2$ km/s, $hf_{SH2} = 4$ km/s, $hf_{SH3} = 6$ km/s. The curves 1, 2, and 3 correspond to values $\sigma_s = 10^{-8}$ S/m, 5×10^{-5} S/m, and 10^{-3} S/m of the layer placed in plane $x_3 = h$, respectively.

3.2. Influence of a layer with arbitrary conductivity on a plate surface on the characteristics of forward and backward SH higher order acoustic waves in X-Y potassium niobate plate

In this paragraph we consider two situations: (i) a layer with arbitrary conductivity is placed in the plane $x_3 = h$ and (ii) above mentioned layer is placed in the planes $x_3 = 0$ and $x_3 = h$. The layer is assumed to be very thin in comparison with the acoustic wavelength so that the effect of mechanical loading can be neglected. As the result of the boundary problem solution described above, we have obtained the dependencies of phase (upper row) and group (middle row) velocities, as well attenuation (lower row) for the forward (Fig. 5) and backward (Fig. 6) SH_1, SH_2, SH_3 acoustic waves at $hf_{SH1} = 2$ km/s, $hf_{SH2} = 4$ km/s, $hf_{SH3} = 6$ km/s propagating in X-Y potassium niobate plate on surface conductivity σ_s. On Figs. 5 and 6 the curves 1 and 2 correspond to situations (i) and (ii), respectively.

The values of attenuation (Γ) in dB/λ were calculated by using the next expression:

$$\Gamma = 4\pi \mathrm{Im}(V_{ph})/(0.23\ \mathrm{Re}(V_{ph})) \tag{12}$$

The group velocities of the corresponding waves have defined by using previously obtained dependencies of phase velocities (V_{ph}) vs surface conductivity, as well calculated analogous dependencies of phase velocities (V^+_{ph}) for parameter $hf^+_{SH1} = 2000.1$ m/s, $hf^+_{SH2} = 4000.1$ m/s, $hf^+_{SH3} = 6000.1$ m/s. Then the next expression was used:

$$V_{gr} = \frac{(V^+_{ph})^2 (hf^+ - hf)}{V_{ph} hf^+ - V^+_{ph} hf}. \tag{13}$$

As it is seen on Fig. 5 for the forward waves the attenuation initially increases, reaches a maximum then falls down with increasing surface conductivity of the layer. It is expected behavior because for very low values of σ_s the layer approximates an ideal dielectric, and for very high values of σ_s it approaches an ideal conductor. In both of these cases, there is no attenuation of the acoustic wave [28]. As for the forward wave phase velocity it decreases with increasing σ_s due to shorting the tangential components of electric field associated with acoustic wave [39].

In contrast to the phase velocity, the group velocity of the forward wave first increases, reaches a maximum, and only then decreases. It can be seen (Fig. 5b, e, and h) that the maximum of the rise corresponds to the maximum of the wave attenuation, and its magnitude is related to the electromechanical coupling coefficient of the waves.

The obtained results have shown the possibility to develop a sensor for the definition of thin film conductivity.

For backward wave one can see an opposite situation on Fig. 6. The phase velocity of this wave increases with increasing σ_s, and attenuation has negative values.

The negative values of attenuation are connected with the fact that the backward waves decay along the plate in the direction of the energy flux which is coincides with group velocity direction.

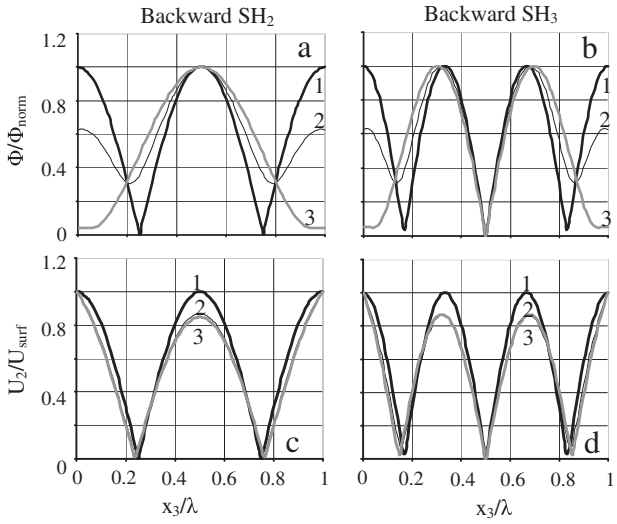

Fig. 9. Dependences of electric potential value (upper row) and maximum mechanical displacement component U_2 (lower row) normalized to the corresponding maximum values for backward SH_2 (a, c), SH_3 (b, d) waves on the thickness of XY $KNbO_3$ plate at $hf_{SH1} = 2$ km/s, $hf_{SH2} = 4$ km/s, $hf_{SH3} = 6$ km/s. The curves 1, 2, and 3 correspond to values $\sigma_s = 10^{-8}$ S/m, 5×10^{-5} S/m, and 10^{-3} S/m of the layers placed in planes $x_3 = 0$ and $x_3 = h$, respectively.

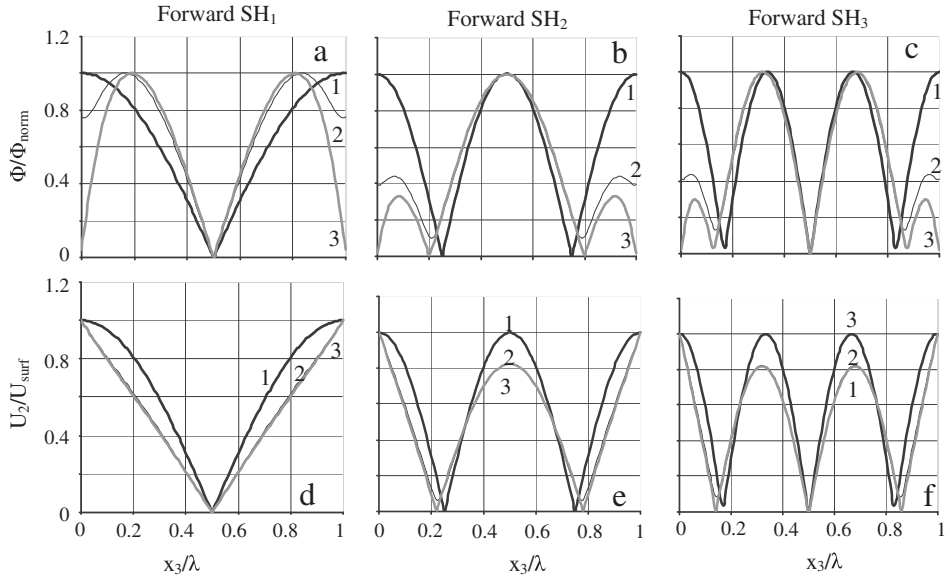

Fig. 10. Dependences of electric potential value (upper row) and maximum mechanical displacement component U_2 (lower row) normalized to the corresponding maximum values for forward SH_1 (a, d), SH_2 (b, e), SH_3 (c, f) waves on the thickness of XY $KNbO_3$ plate at hf_{SH1} = 2 km/s, hf_{SH2} = 4 km/s, hf_{SH3} = 6 km/s. The curves 1, 2, and 3 correspond to values $\sigma_s = 10^{-8}$ S/m, 5×10^{-5} S/m, and 10^{-3} S/m of the layers placed in planes $x_3 = 0$ and $x_3 = h$, respectively.

This behavior is similar with the propagation of the leaky backward acoustic Lamb waves [46].

The dependencies of electric potential value (upper row) and maximum mechanical displacement component U_2 normalized to the value at the plate surface (x_3=0) for the backward (Fig. 7) and forward (Fig. 8) SH_1, SH_2, SH_3 acoustic waves on the plate thickness at hf_{SH1} = 2 km/s, hf_{SH2} = 4 km/s, hf_{SH3} = 6 km/s are presented. The curves 1, 2, and 3 correspond to values $\sigma_s = 10^{-8}$ S/m, 5×10^{-5} S/m, and 10^{-3} S/m of the layer placed in plane $x_3 = h$, respectively.

The dependencies of electric potential value (upper row) and maximum mechanical displacement component U_2 normalized to the corresponding maximum value for backward and forward SH_1, SH_2, SH_3 acoustic waves on the plate thickness at hf_{SH1} = 2 km/s, hf_{SH2} = 4 km/s, hf_{SH3} = 6 km/s are presented on Figs. 9 and 10, respectively. The curves 1, 2, and 3 correspond to values $\sigma_s = 10^{-8}$ S/m, 5×10^{-5} S/m, and 10^{-3} S/m of the layers placed in planes $x_3 = 0$ and $x_3 = h$, respectively.

4. Conclusion

As the result of the study, the dependencies of phase and group velocities for the forward and backward SH acoustic waves propagating in X-Y potassium niobate plate were constructed. The effect of metallization of one or the two sides of the plate on the characteristics of these waves was investigated. The plate metallization was revealed to shift the appearance point for the backward waves into a region of lower frequencies and to essentially increase the range of their existence. The SH_1 backward wave vanishes under metallization of two sides of the plate. It was also noted, that by change of electrical boundary conditions it is possible to control both the magnitude of the potential of electric field associated with the acoustic wave, and the amplitude of particle displacement over the plate thickness. The obtained results have shown the possibility to develop a sensor for the definition of thin film conductivity. For experimental check of the theoretical results it is possible to use mesostructure based on a piezoelectric plate with through nanoholes. Direct measurement of distribution and dynamic change of internal electric field of a wave in a plate can be carried out by means of the electronic probe, for example, of an electronic microscope. By change of the electric boundary conditions on a plate surface it is possible to modulate electronic stream through the piezoelectric plate with nanoholes by means of change of the built-in electric potential over plate depth. A nanoelectronic accelerator (modulator) of electrons based on such principle can be developed.

Acknowledgment

The work has been partially supported by Russian Basic Research Foundation (Grants #16-07-00629, #17-07-00608, #17-57-53101), grant MCMS-0517K03 from SKL of MCMS, Nanjing University of Aeronautics and Astronautics, and grant from NSFC (China) #11611530686.

References

[1] Y. Jin, S.G. Joshi, Excitation of higher-order ultrasonic Lamb wave modes in piezoelectric plates, J. Acoust. Soc. Am. 92 (1992) 914–919.
[2] I.E. Kuznetsova, B.D. Zaitsev, I.A. Borodina, A.A. Teplykh, V.V. Shurygin, S.G. Joshi, Investigation of acoustic waves of higher order propagating in plates of lithium niobate, Ultrasonics 42 (2004) 179–182.
[3] V.I. Anisimkin, N.V. Voronova, I.E. Kuznetsova, I.I. Pyataikin, Aspects of using acoustic plate modes of higher orders for acoustoelectronic sensors, Bull. Russ. Acad. Sci., Phys. 79 (2015) 1278–1282.
[4] B.D. Zaitsev, I.E. Kuznetsova, I.A. Borodina, A.A. Teplykh, The peculiarities of propagation of the backward acoustic waves in piezoelectric plates, IEEE Trans. UFFC 55 (2008) 1660–1664.
[5] P.V. Burlii, P.P. Ilyin, I.Ya. Kucherov, Backward transfer acoustic waves in cubic crystal plates, Acoust. Phys. 43 (1997) 266–270.
[6] S. Bramhavar, C. Prada, A.A. Maznev, A.G. Every, T.B. Norris, T.W. Murray, Negative refraction and focusing of elastic Lamb waves at an interface, Phys. Rev. B 83 (2011) 014106.
[7] F.D. Philippe, T.W. Murray, C. Prada, Focusing on plates: controlling guided waves using negative refraction, Sci. Rep. 5 (2015) 11112.
[8] P.L. Martson, Negative group velocity Lamb waves on plates and applications to the scattering of sound by shells, J. Acoust. Soc. Am. 113 (2003) 2659–2662.
[9] P.V. Burlii, P.P. Ilyin, I.Ya. Kucherov, About possibility existence transversal backward waves in plates, Tech. Phys. Lett. 8 (1982) 568–571.
[10] I.A. Borodina, B.D. Zaitsev, I.E. Kuznetsova, A.A. Teplykh, Hybridization of backward acoustic waves in piezoelectric plates, Tech. Phys. Lett. 34 (2008) 11–13.
[11] I.E. Kuznetsova, I.A. Nedospasov, G.V. Mozhaev, Pure shear backward waves in the X-cut and Y-cut piezoelectric plates of potassium niobate, J. Commun. Technol. Electron. 61 (2006) 1305–1313.

[12] B.D. Zaitsev, I.E. Kuznetsova, I.A. Borodina, S.G. Joshi, Characteristics of acoustic plate waves in potassium niobate ($KNbO_3$) single crystal, Ultrasonics 39 (2001) 51–55.
[13] K. Yamanouchi, H. Odagawa, T. Kojima, T. Matsumura, Theoretical and experimental study of super-high electromechanical coupling surface acoustic waves propagation in $KNbO_3$ single crystal, Electron. Lett. 33 (1997) 193–194.
[14] V.I. Anisimkin, I.I. Pyataikin, N.V. Voronova, Propagation of the Anisimkin Jr'. and quasi-longitudinal acoustic plate modes in low-symmetry crystals of arbitrary orientation, IEEE Trans. UFFC 59 (2012) 806–810.
[15] C. Caliendo, Analytical study of the propagation of fast longitudinal modes along wz-BN/AlN thin acoustic waveguides, Sensors 15 (2015) 2525–2537.
[16] I.S. Didenko, F.S. Hickernell, N.F. Naumenko, The experimental and theoretical characterizarion of the SAW propagation properties for zinc oxide films on silicone carbide, IEEE Trans. UFFC 47 (2000) 179–188.
[17] R.S. Bandhu, X. Zhang, R. Sooryakumar, K. Bussmann, Acoustic vibrations in free-standing double layer membranes, Phys. Rev. B 70 (2004) 075409.
[18] M. Nouh, On the spatial sampling and beat effects in discrete wave profiles of lumped acoustic metamaterials, J. Acoust. Soc. Am. 141 (2017) 1514–1522.
[19] I.E. Kuznetsova, B.D. Zaitsev, E.P. Seleznev, E. Verona, Gasoline identifier based on SH_0 plate acoustic waves, Ultrasonics 70 (2015) 34–37.
[20] K. Sothivelr, F. Bender, F. Josse, A.J. Ricco, E.E. Yaz, R.E. Mohler, R. Kolhatkar, Detection and quantification of aromatic hydrocarbon compounds in water using SH-SAW sensors and estimation-theory-based signal processing, ACS Sensors 1 (2016) 63–72.
[21] V.I. Anisimkin, I.E. Kuznetsova, V.V. Kolesov, I.I. Pyataikin, V.V. Sorokin, D.A. Skladnev, Plate acoustic wave sensoe for detectio of small amounts of bacterial cells in microlitre liquid sample, Ultrasonics 62 (2015) 156–159.
[22] M. Cole, I. Spulber, J.W. Gardner, Surface acoustic wave electronic tongue for robust analysis of sensory components, Sensors Actuat. B-Chem. 207 (2015) 1147–1153.
[23] I.E. Kuznetsova, B.D. Zaitsev, V.I. Anisimkin, A.A. Teplykh, A.M. Shikhabudinov, V.V. Kolesov, V.G. Yakunin, Noncontact determination of thin films conductance by the SH_0 plate acoustic waves, J. Appl. Phys. 115 (2014) 044504.
[24] I.L. Drichko, A.M. Diakonov, V.A. Malysh, I.Yu. Smirnov, E.S. Koptev, A.I. Nikiforov, N.P. Stepina, Y.M. Galperin, J. Bergli, Nonlinear high-frequency hopping conduction in two-dimensional arrays of Ge-in-Si quantum dots: acoustic methods, Solid State Commun. 152 (2012) 860–863.
[25] I.L. Drichko, I.Yu. Smirnov, A.V. Suslov, D.R. Leadley, Acoustic studies of ac conductivity mechanisms in n-GaAs/$Al_xGa_{1-x}As$ in the integer and fractional quantum Hall effect regime, Phys. Rev. B 83 (2011) 235318.
[26] Z.H. Qian, F. Jin, T.J. Lu, K. Kishimoto, Transverse surface waves in a functionally graded piezoelectric substrate coated with a finite-thickness metal waveguide layer, Appl. Phys. Lett. 94 (2009) 023501.
[27] V.I. Anisimkin, N.V. Voronova, M.A. Zemlyanitsyn, I.I. Pyataikin, A.M. Shikhabudinov, The structure of acoustic modes in piezoelectric plates with free and metallized surfaces, J. Comm. Technol. Electron. 57 (2012) 738–742.
[28] B.D. Zaitsev, S.G. Joshi, I.E. Kuznetsova, I.A. Borodina, Influence of conducting layer and conducting electrode on acoustic waves propagating in potassium niobate plates, IEEE Trans. UFFC 48 (2001) 624–626.
[29] I.E. Kuznetsova, S.G. Joshi, B.D. Zaitsev, SH acoustic waves in a lithium niobate plate and the effect of electrical boundary conditions on their properties, Acoust. Phys. 47 (2001) 282–285.
[30] B.D. Zaitsev, I.E. Kuznetsova, S.G. Joshi, I.A. Borodina, Shear horizontal acoustic waves in piezoelectric plates bordered with conductive liquid, IEEE Trans. UFFC 48 (2001) 627–631.
[31] F.L. Guo, G.Q. Wang, Propagation of Bleustein-Gulyaev wave in a piezoelectric crystal in contact with viscous conductive liquids, in: Proceed. of the 2012 Symp. on Piezoel., Acoust. Waves and Device Appl. (SPAWDA12), Shanghai, PR China; 2012. p. 395–8.
[32] B.D. Zaitsev, I.E. Kuznetsova, S.G. Joshi, Influence of electrical boundary conditions on structure of surface acoustic waves in potassium niobate, Electron. Lett. 35 (1999) 1205–1206.
[33] M. Deng, Y. Xiang, Influences of electrical boundary conditions on second-harmonic generation of ultrasonic guided wave propagation in a piezoelectric plate, Phys. Proc. 70 (2015) 356–359.
[34] B.D. Zaitsev, I.E. Kuznetsova, S.G. Joshi, Anomalous resisto-acoustic effect, J. Appl. Phys. 86 (1999) 6868–6874.
[35] B.D. Zaitsev, I.E. Kuznetsova, S.G. Joshi, Anomalous resistoacoustic effect in piezoelectric-conducting liquid structure, Tech. Phys. 46 (2001) 767–769.
[36] I.E. Kuznetsova, B.D. Zaitsev, The peculiarities of the Bleustein-Gulyaev wave propagation in structures containing conductive layer, Ultrasonics 59 (2015) 45–49.
[37] I.E. Kuznetsova, B.D. Zaitsev, The anomalous resisto-acoustic effect in piezoelectric structures with conducting layers, Bull. Russ. Acad. Sci., Phys. 79 (2015) 1288–1292.
[38] A.J. Slobodnik, Jr., E.D. Conway, R.T. Delmonico, Microwave Acoustic Handbook. AFCRL-TR-73-0597; 1973.
[39] B.A. Auld, Acoustic Fields and Waves in Solids, Vols. I and II, John Wiley, New York, 1973.
[40] M. Levy, H. Bass, R. Stern, Modern Acoustical Techniques for the Measurement of Mechanical Properties, vols. 39, Academic Press, 2001.
[41] M. Zgonik, R. Schlesser, I. Biaggio, E. Voit, J. Tscherry, P. Gunter, Material constants of KNbO3 relevant for electro- and acousto-optics, J. Appl. Phys. 74 (1993) 1287–1297.
[42] Z. Hu, H. Cui, Z. An, J. Mao, Measurements of backward wave propagation using the dynamic photoelastic technique, IEEE Ultras. Symp. 1–4 (2016) 1–4.
[43] A.M. Hashim, S. Kasai, T. Hashizume, H. Hasegawa, Large modulation of conductance in interdigital-gated HEMT devices due to surface plasma wave interactions, Jpn. J. Appl. Phys. 44 (2005) 2729–2734.
[44] S.I. Drapak, Z.D. Kovalyuk, The effect of photocurrent amplification in an In_2O_3-GaSe heterostructure, Tech. Phys. Lett. 27 (2001) 755–757.
[45] C. Pakula, V. Zaporojtchenko, T. Strunskus, D. Zargarani, R. Herges, F. Faupel, Reversible light-controlled conductance switching of azobenzene-based metal/polymer nanocomposites, Nanotechnology 21 (2010) 465201.
[46] I.A. Nedospasov, V.G. Mozhaev, I.E. Kuznetsova, Unusual energy properties of leaky backward Lamb waves in a submerged plate, Ultrasonics 77 (2017) 95–99.